A DIRECT X-RAY TECHNIQUE FOR MEASURING MICROFIBRIL ANGLE

M. Lotfy M. El-osta, R. M. Kellogg, R. O. Foschi
Department of the Environment, Canadian Forestry Service
Western Forest Products Laboratory, Vancouver, British Columbia

and

R. G. Butters
Department of Metallurgy, University of British Columbia, Vancouver, B.C.

(Received 27 April 1973)

ABSTRACT

A texture goniometer was utilized for measuring the azimuthal intensity distribution of the (040) meridional diffraction from some coniferous wood tissues. A computerized iterative fitting method was used to generate mathematically the experimental diffraction curve and to resolve the (040) diffraction pattern from the composite profile. The mean microfibril angle was then estimated from the shape of the resolved (040) profile.

The technique developed herein is a direct and simple method for determining the mean microfibril angle with a generally satisfactory level of precision. In addition, the technique is applicable to material with a wide range of microfibril angles.

Additional keywords: Pseudotsuga menziesii, Tsuga heterophylla, meridional diffraction, microfibril angle, X-ray diffraction, (040) peak, numerical analysis, mercury reflectance method, texture goniometer.

INTRODUCTION

Microfibril angle is one of the basic ultrastructural characteristics of woody cell walls. It influences a number of wood properties, such as creep (El-osta and Wellwood 1972), modulus of elasticity (Cowdrey and Preston 1966; Hearle 1963), and dimensional stability (Meylan and Probine 1969). In addition, it exerts primary control on the mechanical properties of single wood pulp fibers (Page et al. 1971). It is therefore of some technological importance to provide wood scientists and technologists with a direct X-ray technique by which microfibril angle can be determined on a routine basis.

Most of the available X-ray techniques for determining the average orientation of cellulose crystallites are based on measurement of the intensity distribution on the paratropic planes, such as (002), ($10\bar{1}$), and (101). This requires interpreting the diffraction patterns to obtain an estimate of the average microfibril angle. The following criteria have been utilized to deduce the mean microfibril angle:

(a) half the angular width of the (002) arc at 40% or 50% of its peak height (Meredith 1951; Preston 1952);
(b) half the angular distance (T) between the points of intersection of the tangents at the inflection points with the zero intensity axis of the (002) diffraction pattern (Cave 1966; El-osta et al. 1972; Meylan 1967).

Criterion (a), which was defined to agree with other experimental results, is invalid in the case of a double-peak (bimodal) diffraction diagram and has no sound theoretical basis. Criterion (b), however, has some theoretical justification, but requires a calibration procedure for conversion of the T angle to microfibril angle (Cave 1966). Different species and wood tissues may also require different calibrations (El-osta et al. 1972; Kellogg et al. 1972).

It is worth mentioning here that other X-ray techniques that utilize the paratropic reflection are available for determining the mean microfibril angle. Among these methods is the one developed by Hermans (1949). Utilizing this method, one can determine the orientation factor and the mean inclination angle of cellulose crystallites to fiber axis. This method has been criticized by DeLuca and Orr (1961) on the grounds that it was designed for regenerated fibers. In general, results derived from paratropic planes are not sufficient to describe the orientation of the b-axis of the cellulose I unit cell.

Diffractions arising from the diatropic (040) plane of cellulose I crystallites give the microfibril angle distribution directly. Unfortunately, this type of diffraction is contaminated at its tails by diffractions from the first and third layer lines and the equator which occur at nearly the same Bragg angle (Mann et al. 1960; Radhakrishnan et al. 1969). Furthermore, this kind of diffraction is usually weaker than the diffraction arising from paratropic planes. However, this difficulty can be overcome by using a tilted specimen as will be shown in the material and methods section of this paper.

A few Japanese scientists have used the (040) diffraction pattern to record the distribution of microfibril angle within the cell wall and to determine the mean angle of some wood species (Nomura and Yamada 1972; Sobue et al. 1971; Suzuki 1967; Watanabe and Inoue 1964). Their analytical approach has two main drawbacks. First, they did not take into consideration the aforementioned contamination of the (040) diffraction pattern of cellulose I. Second, their definition of the background was arbitrary and could produce a certain error in calculating the mean microfibril angle.

The purpose of this paper is:

(1) to illustrate a numerical method for resolving the (040) diffraction pattern from the composite profile;

(2) to utilize the resolved (040) diffraction pattern in calculating the mean microfibril angle.

THEORETICAL APPROACH

Measurement of the intensity of diffraction of a particular plane, as a function of the orientation of a specimen relative to the diffraction vector of a diffractometer, yields information about the preferred orientation of the crystallites in the specimen. Such information is normally presented as a stereographic projection of the plane normals, i.e., a pole-figure diagram. The sum total of all orientation in an oriented specimen is referred to as its texture (Alexander 1969). A useful tool for conducting this kind of study is the texture goniometer.

Geometric considerations of the texture goniometer

Considering the schematic diagram presented in Fig. 1, diffraction will be observed under the following conditions:

(a) Crystallographic planes are present in the specimen and their interplanar spacing satisfies the Bragg equation, i.e.,

$$n\lambda = 2d \sin \theta$$

where: n = order of diffraction;
λ = X-ray wave length;
d = interplanar spacing of the set of planes;
θ = angle between diffraction plane and incident X-ray.

In this work, λ and θ are selected such that d must be 2.6A.

(b) The normals to the planes satisfying (a) must lie in the direction of the diffraction vector OA (in the plane of the paper).

In the case of cellulose I, the various planes satisfying (a) and the angle they make with the (040) plane are as follows (Radhakrishnan et al. 1969):

Plane (hkl)	2θ Angle for Cu Kα (degree)	Angle relative to the (040) (degree)
(040)	34.5	0
(032)	34.0	40.6
(230)		
(113)	34.2	75.4
(013)		
(311)		
(212)		
(310)		
(103)	33.5	90
(003)		
(301)		
(20$\bar{2}$)		
(300)		

If a highly oriented wood specimen with a small microfibril angle is placed at 0 (Fig. 1) and oriented such that the tracheid axis coincides with OA, the detector will measure only diffraction from the (040) planes. Upon rotating the specimen gradually through an azimuthal angle ψ about ON (ON is normal to OA and lies in the plane of the paper), the detector output will quickly fall to the background (BG) because the (040) planes will be so oriented as not to satisfy condition (b) above. As the angle ψ increases to about 40° from the original position, diffraction from the (032) and (230) planes will be recorded,[1] since some of the crystallites in the specimen will have these planes so oriented as to satisfy (a) and (b). Similarly, as ψ approaches 75° and 90°, the detector will register some diffraction from planes of the type (113) and (103), respectively.

In a wood specimen with a lower degree of orientation and broader microfibril angle distribution, the ability to resolve the separate diffractions mentioned above breaks down. The result is a composite profile, the main portion of which is due to diffraction from the (040) plane.

Numerical analysis for resolving (040) diffraction peak

The aim of the numerical analysis used herein is to generate the experimental diffraction diagram mathematically and then resolve the (040) peak from it. Before proceeding further, it is necessary to define the geometry of the technique used. The geometry is as follows (Fig. 2):

(a) The specimen axis is taken parallel to the direction of e_3 (OA in Fig. 1).
(b) The axis of specimen rotation (ON in Fig. 1) is coincident with the direction of e_1.

[1] It is assumed that the microfibril axis coincides with the crystallographic "b" axis (Sisson 1935).

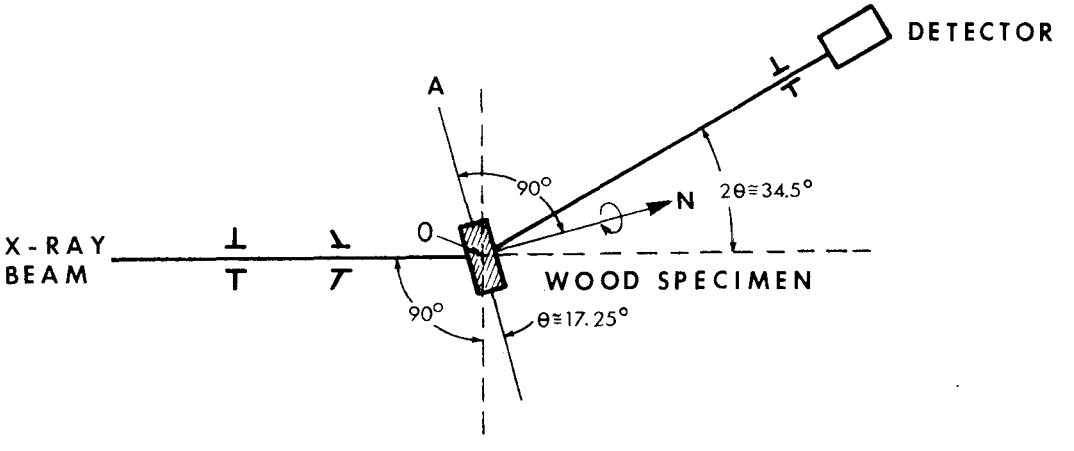

FIG. 1. Conditions for diffraction from the contaminated (040) plane in wood specimen.

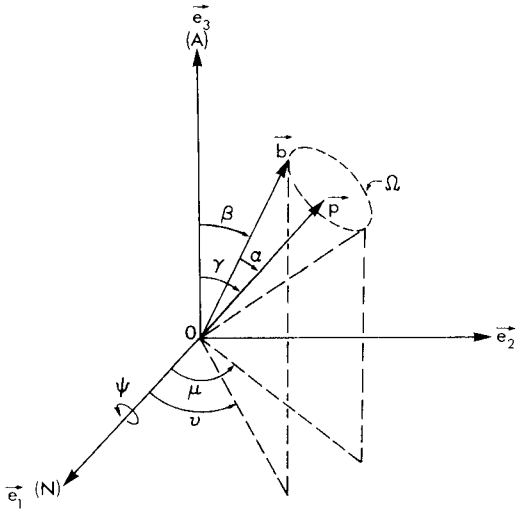

FIG. 2. Geometry of the X-ray technique and the specimen systems.

(c) The microfibril axis direction ($\vec{b}$) is given by the microfibril angle β and the azimuthal angle ν. This direction coincides with the normal to the (040) plane.

(d) There is also another general plane P_α the normal of which ($\vec{P}$) makes an angle α with $\vec{b}$. The direction of $\vec{P}$ is defined by γ and the azimuthal angle μ.

Generally, the unit vector $\vec{P}$ is given by:

$$\vec{P} = \sin\gamma\cos\mu\,\vec{e}_1 + \sin\gamma\sin\mu\,\vec{e}_2 + \cos\gamma\,\vec{e}_3. \quad (1)$$

For the plane P_α to give rise to diffraction, its normal ($\vec{P}$) must become parallel to OA (Fig. 1), through a rotation ψ $\vec{e}_1$. The rotated vector can be written as follows:

$$\vec{P}_r = \sin\gamma\cos\mu\,\vec{e}_1 + [\cos\psi\sin\gamma\sin\mu - \sin\psi\cos\gamma]\,\vec{e}_2 + [\sin\psi\sin\gamma\sin\mu + \cos\psi\cos\gamma]\,\vec{e}_3. \quad (2)$$

Accordingly, the diffraction occurs when the components in the directions of $\vec{e}_1$ and $\vec{e}_2$ become zero, i.e.:

$$\sin\gamma\cos\mu = 0 \quad \text{and} \quad (3)$$
$$\cos\psi\sin\gamma\sin\mu - \sin\psi\cos\gamma = 0. \quad (4)$$

To satisfy equation (3), for the general case of $\gamma \neq 0$.

$$\cos\mu = 0 \quad \text{or} \quad \mu = \pi/2, 3\pi/2. \quad (5)$$

From equations (5) and (4),

$$\sin(\psi \pm \gamma) = 0. \quad (6)$$

Thus, the rotation that is required to bring P_α plane in a position for diffraction is given by

$$\psi = \pm\gamma \pm n\pi \quad (7)$$
where: $n = 0, 1, \ldots$.

Equations (5) and (7) can be utilized to construct the components of the diffraction profiles produced by planes having Bragg's angle near 17.25°.

1. Plane (040)

In this case, $\alpha = 0$, $\gamma = \beta$ and $\mu = \nu$. Application of equation (5) indicates that the diffraction from the (040) plane is possible only from microfibrils in planes normal to the direction ON (Fig. 1). This condition, whereby the X-ray beam falls on the tangential face of the wood specimen, is satisfied by:

(a) microfibrils in the tangential walls of the specimen,

(b) microfibrils having zero angle in the radial walls and

(c) if, through weaving in and out of the plane of the radial walls, some microfibrils lie in a plane parallel to the plane of rotation. However, contribution to diffraction profile from these microfibrils is probably small and would not materially affect the result.

According to equation (7), the required specimen rotation for a given microfibril with an angle β is:

$$\psi = \pm\beta \pm n\pi. \quad (8)$$

2. General plane P_α

In the general case, the plane P_α is defined as making an angle α with the plane (040). However, there exists an infinite number of directions that make an angle α with $\vec{P}$. This family of directions gener-

ates a conical surface Ω (Fig. 2). The vector $\vec{b}$ can be expressed in the following manner:

$$\vec{b} = \sin\beta\cos\nu\,\vec{e}_1 + \sin\beta\sin\nu\,\vec{e}_2 + \cos\beta\,\vec{e}_3; \quad (9)$$

and, if P_α is in a position to satisfy the condition for diffraction, the vector $\vec{P}$ can be written as follows, according to equations (1) and (5):

$$\vec{P} = \pm\sin\gamma\,\vec{e}_2 + \cos\gamma\,\vec{e}_3. \quad (10)$$

Since the family of vectors $\vec{b}$ on the surface Ω satisfies the condition:

$$\vec{P}\cdot\vec{b} = \cos\alpha, \quad (11)$$

the following relationship is obtained:

$$\cos\alpha = \pm\sin\gamma\sin\beta\sin\nu + \cos\beta\cos\gamma. \quad (12)$$

Let us consider the case whereby an X-ray beam falls on the tangential face of a wood specimen:

a: *For microfibrils located in one pair of tangential walls ($\nu = \pi/2,\ 3\pi/2$, Fig. 2)*

For those walls equation (12) becomes:

$$\cos\alpha = \cos(\beta - \gamma), \quad (13)$$

$$\text{from which } \gamma = \beta \pm \alpha, \quad (14)$$

and according to equation (7) the required rotation for producing diffraction from the P_α plane of these microfibrils is given by:

$$\psi = \beta \pm \alpha \pm n\pi \text{ for } \nu = \pi/2, \text{ and} \quad (15)$$
$$\psi = -\beta \pm \alpha \pm n\pi \text{ for } \nu = 3\pi/2,$$
where: $n = 0, 1, \ldots$.

b: *For microfibrils located in one pair of radial walls*[2] *($\nu = \pi, 2\pi$)*

For those walls equation (12) becomes:

$$\cos\alpha = \cos\beta\cos\gamma \quad (16)$$

and according to equation (7) the required rotation for producing diffraction from the P_α plane of these microfibrils is given by:

$$\psi = \pm\arccos(\cos\alpha/\cos\beta) \pm n\pi \quad (17)$$
where: $n = 0, 1, \ldots$.

c: *For microfibrils located in walls with ν other than $\pi/2$, π, $3\pi/2$, or 2π.*

Equation (7) and (12) can again be used to determine the required rotation for producing diffraction from the P_α plane for those microfibrils. Equation 12, however, becomes in this case a transcendental equation for γ and cumbersome to solve. For simplicity, this contribution to the diffraction profile will not be considered here. This approximation is equivalent to taking the cross section of the tracheid to be rectangular in shape. Since the true shape is not precisely known, a more precise model is not required. This approximation is not expected to significantly affect the results since it is related only to minor contributions from planes other than (040).

Limiting the angles ψ, β, and α to values between 0 and $\pi/2$, the composite diffraction profile at ψ can now be obtained by superposition of results derived from equations (8), (15), and (17). This profile consists of diffraction from:

(a) (040) plane of microfibrils in tracheid tangential wall ($\nu = \pi/2$) and and also in the radial wall for $\beta = 0$ with:

$$\beta = \psi \quad (18)$$

(b) P_α plane of microfibrils in the tracheid tangential wall at ($\nu = \pi/2$) with:

1. $\beta = \psi - \alpha$ if $\psi \geq \alpha$
2. $\beta = \psi + \alpha$ if $\psi + \alpha \leq \pi/2$ (19)

(c) P_α plane of microfibrils in the tracheid tangential wall ($\nu = 3\pi/2$) with:

1. $\beta = \alpha - \psi$ if $\psi < \alpha$
2. $\beta = \pi - (\psi + \alpha)$ if $\psi + \alpha > \pi/2$ (20)

(d) P_α plane of microfibrils in the tracheid radial walls ($\nu = \pi,\ 2\pi$) with $\beta = \arccos(\cos\alpha/\cos\psi)$ if $\psi \leq \alpha$ (21)

[2] The authors wish to thank Dr. F. El-Hosseiny of the PPRIC for his useful comments.

Thus, if

$I_4(\beta) = (040)$ intensity distribution as a function of the microfibril angle β,

$I_\alpha(\beta) = P_\alpha$ intensity distribution as a function of β,

$I(\psi)$ = intensity distribution as a function of ψ, and considering that the three groups of planes occur at $\alpha_1 = 40.6°$, $\alpha_2 = 75.4°$ and $\alpha_3 = 90°$ from (040) plane, then the observed composite intensity at ψ can be written as follows:

$$\begin{aligned} I(\psi) = {} & I_4(\psi) \\ & + \sum_{i=1}^{2} \Big\{ I_{\alpha_i}(\psi - \alpha_i)\,\Delta(\psi - \alpha_i) \\ & \quad + I_{\alpha_i}(\alpha_i - \psi)\,\Delta(\alpha_i - \psi) \\ & \quad + I_{\alpha_i}(\psi + \alpha_i)\,\Delta[\pi/2 - (\psi + \alpha_i)] \\ & \quad + I_{\alpha_i}[\pi - (\psi + \alpha_i)]\,\Delta(\psi + \alpha_i) - \pi/2] \\ & \quad + I_{\alpha_i}\left[\arccos\left(\frac{\cos\alpha}{\cos\psi}\right)\right]\Delta^*(\alpha_i - \psi)\Big\} \\ & + I_{\alpha_3}(\pi/2 - \psi) + I_{\alpha_3}(\pi/2) \quad . \end{aligned} \tag{22}$$

where the step functions $\Delta(x)$ and $\Delta^*(x)$ are defined in the following manner:

$$\begin{aligned} &\Delta(x) = 1 \quad \text{if } x > 0 \\ &\Delta(x) = 1/2 \quad \text{if } x = 0 \\ &\Delta(x) = 0 \quad \text{if } x < 0 \\ &\Delta^*(x) = 1 \quad \text{if } x \geq 0 \\ &\Delta^*(x) = 0 \quad \text{if } x < 0. \end{aligned} \tag{23}$$

Assuming that the intensity distribution function I_4 and, in general, I_α are Gaussian centered at angle β_0, corresponding to the greatest density of microfibrils, then these distributions can be expressed by:

$$\begin{aligned} I_4(\beta) &= H_1^2 e^{-H_2^2(\beta - \beta_0)^2} \\ I_{\alpha_1}(\beta) &= H_3^2 e^{-H_4^2(\beta - \beta_0)^2} \\ I_{\alpha_2}(\beta) &= H_5^2 e^{-H_6^2(\beta - \beta_0)^2} \\ I_{\alpha_3}(\beta) &= H_7^2 e^{-H_8^2(\beta - \beta_0)^2} \end{aligned} \tag{24}$$

Substituting equations (24) into equation (22) gives the intensity observed at specimen rotation angle ψ as a function of the parameters H_1^2 through H_8^2 and β_0:

$$\begin{aligned} I(\psi) = {} & H_1^2 e^{-H_2^2(\psi - \beta_0)^2} \\ & + H_3^2 \Big\{ e^{-H_4^2(\psi - \alpha_1 - \beta_0)^2}\,\Delta(\psi - \alpha_1) \\ & \quad + e^{-H_4^2(\alpha_1 - \psi - \beta_0)^2}\,\Delta(\alpha_1 - \psi) \\ & \quad + e^{-H_4^2(\psi + \alpha_1 - \beta_0)^2}\,\Delta[\pi/2 - (\psi + \alpha_1)] \\ & \quad + e^{-H_4^2[\pi - (\psi + \alpha_1) - \beta_0]^2}\,\Delta[\psi + \alpha_1 - \pi/2] \\ & \quad + e^{-H_4^2\left[\arccos\left(\frac{\cos\alpha}{\cos\psi}\right) - \beta_0\right]^2}\,\Delta^*(\alpha_1 - \psi)\Big\} \\ & + H_5^2 \Big\{ e^{-H_6^2(\psi - \alpha_2 - \beta_0)^2}\,\Delta(\psi - \alpha_2) \\ & \quad + e^{-H_6^2(\alpha_2 - \psi - \beta_0)^2}\,\Delta(\alpha_2 - \psi) \\ & \quad + e^{-H_6^2(\psi + \alpha_2 - \beta_0)^2}\,\Delta[\pi/2 - (\psi + \alpha_2)] \\ & \quad + e^{-H_6^2[\pi - (\psi + \alpha_2) - \beta_0]^2}\,\Delta[\psi + \alpha_2 - \pi/2] \\ & \quad + e^{-H_6^2\left[\arccos\left(\frac{\cos\alpha}{\cos\psi}\right) - \beta_0\right]^2}\,\Delta^*(\alpha_2 - \psi)\Big\} \\ & + H_7^2 \Big\{ e^{-H_8^2(\pi/2 - \psi - \beta_0)^2} + e^{-H_8^2(\pi/2 - \beta_0)^2} \Big\} . \end{aligned} \tag{25}$$

The model used herein differs from that employed by Radhakrishnan et al. (1969) in that they assumed that all intensity distribution functions of equations (24) had the same shape and differed only by a scale factor. This assumption required the use of only five parameters in their equation. It was both their observation and ours that this is too restrictive and contrary to experience. In addition they did not take into consideration the contribution to their diffraction profile from microfibrils located in the other walls (i.e. radial wall in this study).

The parameters H_1^2 through H_8^2 and β_0 can be computed by a nonlinear least-squares method of fit. Thus, if $I_D(\psi_i)$ is the observed intensity for an angle of ψ_i, the parameters can be computed from the condition that

$$U = \sum_{i=1}^{NA} \{[I_D(\psi_i) - BG(\psi_i)] - I(\psi_i)\}^2 \tag{26}$$

be a minimum, where NA is the number of observations, $BG(\psi_i)$ is the background, and $I(\psi_i)$ is the net intensity calculated by

equation (25) at angle ψ_i. The minimization of U can be achieved by using Fletcher and Powell's method (1963). It should be indicated that H_1 through H_8 are unconstrained since their squares are used in equations (24), considering that the parameters of the Gaussian distributions have to be positive. In order to make the search for the optimum angle β_0 unconstrained also, H_9 was defined such that $\beta_0 = H_9^2$.

Having evaluated H_1 and H_2 numerically, one can generate the resolved (040) diffraction pattern as a function of β, from which the mean microfibril angle can be calculated.

MATERIALS AND METHODS

Wood specimens of Douglas-fir [*Pseudotsuga menziesii* (Mirb.) Franco] and western hemlock [*Tsuga heterophylla* (Raf.) Sarg.] were chosen from available stock in the Western Forest Products Laboratory. A total of 16 specimens having dimensions 1.0–1.5 mm radially, 1.0 cm tangentially, and 1.0 cm longitudinally were machined from earlywood and latewood zones. Since the specimen edge was used as a reference for mounting in the texture goniometer, care was taken to ensure a cut parallel to the grain. Optimum specimen thickness can be calculated according to standard techniques (Alexander 1969). Considering differences in tissue density, these calculations and practical experience led to the adoption of an optimum thickness of 1.0 mm and 1.5 mm for latewood and earlywood specimens, respectively.

Phillips P. W. 1009 X-ray diffraction apparatus and Phillips P. W. 1078 texture goniometer used in the transmission mode were utilized in this study. Nickel-filtered Cu X-ray generated at 35 kV and 13 mA were employed. The diffracted intensities were determined by means of a proportional counter, pulse-height analyzer, and scaler.

A wood specimen was placed in position 0 (Fig. 1) and set to oscillate 6 mm transverse to the X-ray beam. The beam penetrated the tangential face of the specimen. The (040) and background intensities were determined at 2θ angles of 34.5° and 30°, respectively. The intensity of the background angle was found to be substantially free of reflections at any azimuthal angle. Peak and background intensities were determined at 5° azimuthal increments from $\psi = -90°$ to $+90°$ using 10 seconds counting time. It is recognized that an increased counting time would be expected to improve counting precision. However, experience with a 20-second counting time did not appear to significantly affect the mean microfibril angle, but did appreciably increase the time required for data collection.

Analytical procedure

For the purpose of conducting the numerical analysis, a computer program[3] was written to fit equation (25) to the experimental results. Prior to the curve-fitting procedure, the intensities from $\psi = -90°$ to $+90°$ were checked for symmetry about $\psi = 0°$, to verify the correct positioning of the specimen in the texture goniometer. Using the function

$$V = \sum_{i=1}^{NP} \left\{ [I_D(-\psi_i) - BG(-\psi_i)] - [I_D(\psi_i) - BG(\psi_i)] \right\}^2 \quad (27)$$

where: NP = number of data points considered, a test was run to find the origin for the angles ψ for which V is a minimum. The angle satisfying this condition was considered to be the best approximation to the symmetry point at which the origin $\psi = 0$ must be located. Then the intensities for $+\psi$ angles are added to those for the symmetric $-\psi$ angles and averaged to give the best estimate for the mean intensities for $\psi = 0$ to $\psi = 90°$.

It was necessary to provide initial estimates of the value of H_1^2 in order to start the iterative procedure in the minimization algorithm. Since diffraction arising from (040) plane constitutes the main part of

[3] The program is available from the Western Forest Products Laboratory, 6620 N.W. Marine Drive, Vancouver 8, B.C. (Information Report VP-X-114).

the composite profile, H_1^2 was approximated by the actual maximum intensity observed. The location of this maximum was considered as the first approximation to β_0 which, in turn, was taken as the initial estimate for H_9^2.

Differentiating $I_4(\beta)$ in equations (24) and letting $\beta = \beta_0$, the following equation was obtained for calculating H_2^2:

$$H_2^2 = \frac{-I''_4(\beta_0)}{2H_1^2} \qquad (28)$$

$I''_4(\beta_0)$, the second derivative of I_4, was estimated by the curvature of a parabola fitted to the intensity data in an interval with center at $\beta = \beta_0$.

For diffractions due to planes occurring at α_1, α_2, and α_3 from the (040) plane, it was assumed initially that the parameters H_3^2, H_5^2, and H_7^2 were only 0.10 H_1^2. In addition, as a first approximation, the shape of all intensity functions in equations (24) was considered to be the same, i.e. each of H_4^2, H_6^2 and H_8^2 equals H_2^2. It is important also for numerical stability that data be available at the peaks of the different Gaussian distributions. This condition was not always met during the unconstrained search for the optimum β_0. Therefore, extra data points were interpolated if required during the minimization process.

Calculation of the mean microfibril angle

Assuming that the intensity distribution function $I_4(\beta)$ changes only by a scale factor if the specimen is rotated about the longitudinal tracheid axis, the mean microfibril angle $<\beta>$ can be calculated as follows (Sobue et al. 1971):

$$<\beta> = \frac{\int_0^{\pi/2} \beta\, I_4(\beta) \sin\beta\, d\beta}{\int_0^{\pi/2} I_4(\beta) \sin\beta\, d\beta}. \qquad (29)$$

The integrals are evaluated numerically after the parameters H_1^2 and H_2^2 have been computed and the function I_4 is known from equations (24). The magnitude of $I_4(\beta)$, for a given counting time, will be dependent upon the cross-sectional shape of the tracheid. However, this will not affect the mean microfibril angle according to equation (29).

It was desirable to compare the mean microfibril angle obtained by the X-ray technique with that obtained by a direct microscopic method. For this purpose, the mean microfibril angle was determined by the mercury reflectance method (Page 1969) on the tangential surface of the same specimens used in the X-ray study. Details of the method and specimen preparation, used herein, are similar to those outlined recently by El-osta et al. (1972).

RESULTS AND DISCUSSION

The numerical iterative procedure outlined above was applied to the azimuthal intensity scannings of 16 wood specimens. Considerable success was achieved in fitting equation (25) to the experimental results. Coefficients of determinations for the 16 specimens ranged from 0.852 to 0.998. The results of the numerical analyses are shown in Fig. 3 for three selected specimens. In this figure, the resolved (040) profiles (curves C) indicate a spectrum of shapes ranging from sharp (unimodal) for western hemlock earlywood specimen WHEW-A (Fig. 3-a) to less sharp (unimodal) for Douglas-fir earlywood specimen DFEW-C (Fig. 3-b), or broad (bimodal) for specimen DFEW-G (Fig. 3-c).

Numerical estimates of the parameters of diffraction patterns presented in this paper were obtained with an absolute accuracy of 0.5 for the parameters H_1^2 to H_8^2 and 0.2° for H_9^2. A computation time in the range of 2.48–8.97 seconds, depending on the number of iterations, was needed on an IBM 360/67. It was found that greater accuracy requirements increased the computation time without significantly affecting the mean microfibril angle.

Mean values of the microfibril angle deduced from the X-ray technique by applying equation (29) to the resolved (040) profiles are shown in Table 1. As a check on the reproducibility of these values, 11 azimuthal intensity scannings were taken for specimens DFEW-G and DFEW-F

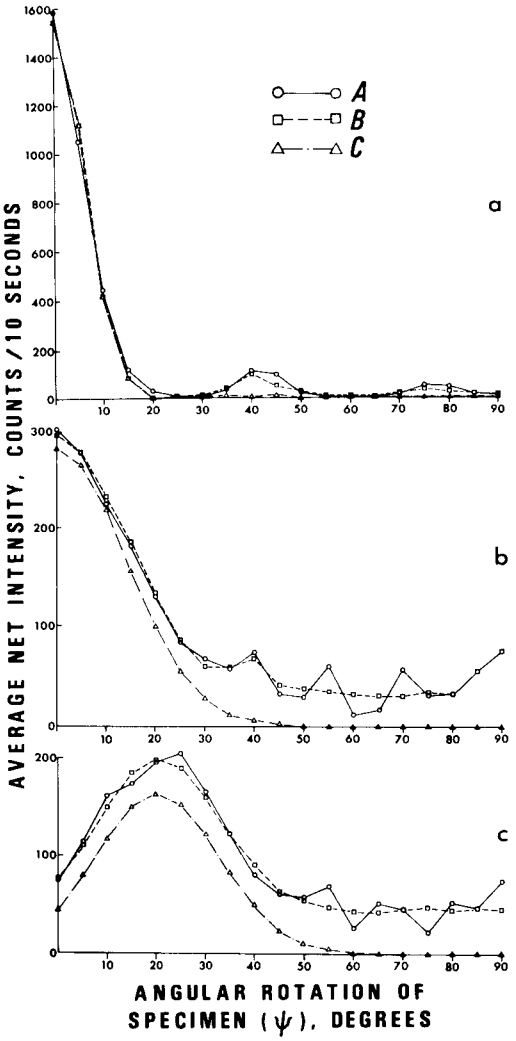

FIG. 3. Azimuthal profiles of (040) diffraction from, a. WHEW-A, b. DFEW-C and c. DFEW-G, A = Composite experimental profile, B = Composite calculated profile, C = Resolved (040) profile.

without removing the specimen from the texture goniometer. Another 11 scannings were made on DFEW-F after remounting the specimen between each scan. The results of statistical analysis showed that the coefficient of variation in the mean microfibril angle was about 7%, with no additional variance component due to remounting. Recognizing the fact that the total random error in measuring the intensity depends upon counting statistics (the random distribution of X-ray counts taken repeatedly at one point follows a Poisson distribution) and generator and X-ray tube stability, the above-noted coefficient of variation would be expected.

TABLE 1. *Mean values of microfibril angle as estimated by X-ray technique and by mercury reflectance method.*

Sample type[1]	X-ray technique (degree)	Mercury reflectance[2] (degree)
DFEW-A	20.1	21.8 (4.5)
DFEW-B	15.6	21.5 (5.4)
DFEW-C	17.4	18.6 (4.2)
DFEW-D	21.0	21.8 (3.5)
DFEW-E	22.2	27.1 (4.1)
DFEW-F	19.8	20.0 (3.8)
DFEW-G	27.3	28.2 (3.4)
DFLW-A	11.4	13.9 (4.3)
DFLW-B	12.4	14.9 (4.0)
DFLW-C	10.7	13.9 (3.3)
DFLW-D	13.0	15.5 (5.3)
DFLW-E	18.4	15.8 (3.1)
WHEW-A	8.2	7.7 (2.6)
WHEW-B	8.3	7.5 (2.8)
WHEW-C	8.6	7.8 (1.9)
WHEW-D	9.0	9.1 (2.1)

[1] DF = Douglas-fir
WH = Western Hemlock
EW = Earlywood
LW = Latewood

[2] Values presented in this column are mean values (based upon 20 measurements) and associated standard deviations.

The mean values of microfibril angle determined by the mercury reflectance method on the same specimen are shown in Table 1.

Considering the difference in physical principles employed by these two techniques, it seems apparent that, at least for the materials examined, the two methods are direct estimates of the same parameter. The X-ray technique outlined here does not require the use of a calibration curve, is averaged over a significant volume of the specimen, is nondestructive, simple, and fast. The complete data collection for one specimen can be obtained in 30 minutes with the apparatus employed.

It should be indicated here that El-Hosseiny and Page (1973) have recently reported that the determination of microfibril angle by mercury reflectance method

must be used with caution because of the error that might be induced by the birefringence of S_1 and S_3 layers. The error is small ($<1°$) for tracheids with thin S_1 and S_3 layers (<0.2 μm) and S_2 layer in the range 1.3–3.4 μm. Fortunately, the tracheids of most softwoods lie within this range.

The steps required, in practice, for obtaining the mean microfibril angle are summarized here. First, using a texture goniometer, an azimuthal scanning of the composite diffraction profile can be obtained. Next, the computer program can be used to fit equation (25) to experimental data, and the resolved (040) diffraction patterns can then be deduced. Finally, the mean microfibril angle can be calculated by equation (29).

SUMMARY AND CONCLUSIONS

A direct X-ray technique to determine the mean microfibril angle in wood is outlined. The variation of azimuthal intensity of the resolved (040) diffraction peak was utilized to determine the mean microfibril angle in some earlywood and latewood specimens of Douglas-fir and western hemlock. A method of numerical analysis is devised by which the (040) diffraction pattern can be resolved from the composite profile. The results of applying the numerical analysis to 16 wood specimens of two coniferous species indicated that the analysis can be applied to widely variable azimuthal profiles.

The proposed X-ray technique is a direct and accurate method for determining the mean microfibril angle. The precision of the estimate probably is limited by the nature of counting statistics and instrument stability.

REFERENCES

ALEXANDER, L. 1969. X-ray diffraction methods in polymer science. John Wiley, New York. 582 pp.

CAVE, I. D. 1966. Theory of X-ray measurement of microfibril angle in wood. For. Prod. J. 16(10):37–42.

COWDREY, D. R., AND R. D. PRESTON. 1966. Elasticity and microfibrillar angle in the wood of Sitka spruce. Proc. Roy. Soc. (London) B 166:245–272.

DELUCA, L. B., AND R. S. ORR. 1961. Crystallite orientation and spiral structure of cotton. Part 1. Native cottons. J. Polymer Sci. 54:457–470.

EL-HOSSEINY, F., AND D. H. PAGE. 1973. The measurement of fibril angle of wood fiber using polarized light. Submitted to Wood and Fiber.

EL-OSTA, M. LOTFY M., AND R. W. WELLWOOD. 1972. Short-term creep as related to microfibril angle. Wood Fiber 4(1):26–32.

———, ———, ———, AND R. G. BUTTERS. 1972. An improved X-ray technique for measuring microfibril angle of coniferous wood. Wood Sci. 5(2):113–117.

FLETCHER, R., AND M. POWELL. 1963. A rapidly convergent descent method for minimization. Comput. J. 6:163–168. (FMFP routine in IBM's Scientific Package).

HEARLE, J. W. S. 1963. The fine structure of fibers and crystalline polymers. III. Interpretation of the mechanical properties of fibers. J. Appl. Polymer Sci. 7:1207–1223.

HERMANS, P. H. 1949. Physics and chemistry of cellulose fibers. Elsevier, New York. 534 pp.

KELLOGG, R. M., J. GONZALEZ, AND B. A. MEYLAN. 1972. Some observations on techniques of measuring fibril angle. Can. Forest. Serv., Western For. Prod. Lab., Vancouver, B.C. (Paper presented to 26th Annual Meeting For. Prod. Res. Soc., Dallas, Texas, June 18–23).

MANN, L., L. ROLDAN-GONZALEZ, AND H. J. WELLWARD. 1960. Crystalline modifications of cellulose. Part IV. Determination of X-ray intensity data. J. Polymer Sci. 42:165–171.

MEREDITH, R. 1951. On the technique of measuring orientation in cotton by X-rays. J. Textile Inst. 42:T275–290.

MEYLAN, B. A. 1967. Measurement of microfibril angle by X-ray diffraction. For. Prod. J. 17(5):51–58.

———, AND M. C. PROBINE. 1969. Microfibril angle as a parameter in timber quality assessment. For. Prod. J. 19(4):30–34.

NOMURA, T., AND T. YAMADA. 1972. Structural observation on wood and bamboo by X-ray. Wood Res. (Japan) 52:1–12.

PAGE, D. H. 1969. A method for determining the fibrillar angle in wood tracheids. J. Microscopy 90(10):137–143.

———, F. EL-HOSSEINY, K. WINKER, AND R. BAIN. 1971. The mechanical properties of single wood pulp fibers. Part 1: A new approach. Pulp Pap. Mag. Can. 73(8):T198–203.

PRESTON, R. D. 1952. The molecular architecture of plant cell walls. Chapman and Hall, London. 176 pp.

RADHAKRISHNAN, T., N. B. P. PATIL, AND N. E. DWELTZ. 1969. Crystalline orientation in natural cellulose fibers. Textile Res. J. 39: 1003–1014.

SISSON, W. A. 1935. X-ray studies of crystallite

orientation in cellulose fibers. Ind. Eng. Chem. 27:51–56.

SOBUE, N., N. HIRAI, AND I. ASANO. 1971. Studies on structure of wood by X-ray. II. Estimation of the orientation of micells in cell wall. J. Jap. Wood Res. Soc. 17(2):44–50.

SUZUKI, M. 1967. The relationship between elasticity and strength properties and cell wall studies of coniferous wood. Bull. Govt. For. Exp. Sta. (Japan) 212:89–149.

WATANABE, S., AND S. INOUE. 1964. Spiral angle of cellulose fiber. Kogyo Kagaku Zasshi (Tokyo) 64(1):42–44.

Page 1

U. S. POSTAL SERVICE

STATEMENT OF OWNERSHIP, MANAGEMENT AND CIRCULATION

(Act of August 12, 1970: Section 3685, Title 39, United States Code)

SEE INSTRUCTIONS ON PAGE 2 (REVERSE)

1. TITLE OF PUBLICATION: **Wood and Fiber**

2. DATE OF FILING: **10/1/73**

3. FREQUENCY OF ISSUE: **Quarterly**

4. LOCATION OF KNOWN OFFICE OF PUBLICATION *(Street, city, county, state, ZIP code) (Not printers)*: **P.O. Box 5062, Madison, WI 53705**

5. LOCATION OF THE HEADQUARTERS OR GENERAL BUSINESS OFFICES OF THE PUBLISHERS *(Not printers)*: **P.O. Box 5062, Madison, WI 53705**

6. NAMES AND ADDRESSES OF PUBLISHER, EDITOR, AND MANAGING EDITOR

PUBLISHER *(Name and address)*: **Allen Press, P.O. Box 368, Lawrence, KA 66044**

EDITOR *(Name and address)*: **Robert W. Meyer, Forest Products Laboratory, 6620 N.W. Marine Dr., Vancouver 8, B.C.**

MANAGER EDITOR *(Name and address)*: **Robert W. Meyer, Forest Products Laboratory, 6620 N.W. Marine Dr., Vancouver 8, B.C.**

7. OWNER *(If owned by a corporation, its name and address must be stated and also immediately thereunder the names and addresses of stockholders owning or holding 1 percent or more of total amount of stock. If not owned by a corporation, the names and addresses of the individual owners must be given. If owned by a partnership or other unincorporated firm, its name and address, as well as that of each individual must be given.)*

NAME	ADDRESS
Society of Wood Science and Technology	**P.O. Box 5062, Madison, WI 53705**

8. KNOWN BONDHOLDERS, MORTGAGEES, AND OTHER SECURITY HOLDERS OWNING OR HOLDING 1 PERCENT OR MORE OF TOTAL AMOUNT OF BONDS, MORTGAGES OR OTHER SECURITIES *(If there are none, so state)*

NAME	ADDRESS
None	

9. FOR OPTIONAL COMPLETION BY PUBLISHERS MAILING AT THE REGULAR RATES (Section 132.121, Postal Service Manual)

39 U. S. C. 3626 provides in pertinent part: "No person who would have been entitled to mail matter under former section 4359 of this title shall mail such matter at the rates provided under this subsection unless he files annually with the Postal Service a written request for permission to mail matter at such rates."

In accordance with the provisions of this statute, I hereby request permission to mail the publication named in Item 1 at the reduced postage rates presently authorized by 39 U. S. C. 3626

(Signature and title of editor, publisher, business manager, or owner) **VON L. BYRD, Executive Secretary**

10. FOR COMPLETION BY NONPROFIT ORGANIZATIONS AUTHORIZED TO MAIL AT SPECIAL RATES *(Section 132.122, PostalManual)* *(Check one)*

The purpose, function, and nonprofit status of this organization and the exempt status for Federal income tax purposes: ☒ Have not changed during preceding 12 months ☐ Have changed during preceding 12 months *(If changed, publisher must submit explanation of change with this statement.)*

11. EXTENT AND NATURE OF CIRCULATION	AVERAGE NO. COPIES EACH ISSUE DURING PRECEDING 12 MONTHS	ACTUAL NUMBER OF COPIES OF SINGLE ISSUE PUBLISHED NEAREST TO FILING DATE
A. TOTAL NO. COPIES PRINTED *(Net Press Run)*	1,000	1,000
B. PAID CIRCULATION 1. SALES THROUGH DEALERS AND CARRIERS, STREET VENDORS AND COUNTER SALES	0	0
2. MAIL SUBSCRIPTIONS	757	761
C. TOTAL PAID CIRCULATION	757	761
D. FREE DISTRIBUTION BY MAIL, CARRIER OR OTHER MEANS 1. SAMPLES, COMPLIMENTARY, AND OTHER FREE COPIES	16	16
2. COPIES DISTRIBUTED TO NEWS AGENTS, BUT NOT SOLD	0	0
E. TOTAL DISTRIBUTION *(Sum of C and D)*	773	777
F. OFFICE USE, LEFT-OVER, UNACCOUNTED, SPOILED AFTER PRINTING	227	223
G. TOTAL *(Sum of E & F should equal net press run shown in A)*	1,000	1,000

▶ *(Signature of editor, publisher, business manager, or owner)*

I certify that the statements made by me above are correct and complete

PS Form 3526 July 1971